Phase change materials as integrated functional components in modern electroceramics

Piotr Zachariasz, Bartłomiej Sikora, Elżbieta Szostak, Radosław Cichocki, and Beata Synkiewicz-Musialska

Abstract—**Cordierite and Li₂CuPO₄ synthesis were endeavored using the solid-phase reaction or wet chemistry methods. Excellent microencapsulation of the [Erythritol]-HDPE composite was demonstrated, while the [Luxolina]-TEOS system exposes low affinity to the core-shell structure. The thermal properties of electroceramics and PCM (phase change material) composite were characterized by the heating rate index (f_h), heating lag factor (j_h), and temperature stability time (t_s).**

Keywords—**electroceramics; phase-change materials; thermo-regulators; thermal conductivity**

I. INTRODUCTION

PHASE-CHANGE materials (PCMs) can absorb extensive thermal energy per unit mass at temperatures near their phase transitions [1]-[5]. Although the PCM temperature does not significantly modify during heat energy accumulation, the phenomenon most often involves a solid-liquid phase transition. The above requires PCM shielding with a more thermally resistant encapsulator to prevent the PCM loss at the liquid phase [6],[7]. Hence, e.g., ceramic microcapsules [8],[9] reveal some temperature discrepancies relative to the surroundings at thermal energy transfers.

It is commonly known that typical polycrystalline ceramics are characterized by a relatively low thermal conductivity of $1 \div 30$ W·m^{-1}·K^{-1} [10],[11] with respect, e.g., to metals, alloys, or advanced nanocarbon structures ($100 \div 5000$ W·m^{-1}·K^{-1}) [12], [13]. Therefore, PCMs are poorly suited for high-performance heating/cooling systems such as Peltier units or temperature-effectively reducing modules dedicated to electronics components strongly radiating Joule heat [14].

Nevertheless, PCMs are expected to operate efficiently as passive cooling elements (supporting thermal heat dissipation) in applications without intense temperature gradients [15] or systems with instantaneously generated heat, e.g., pulse lasers/masers operating in short-period manners [16],[17].

The residential construction industry is an example of the first-mentioned PCM implementation since the insulating facility materials can slowly accumulate solar heat and then release it at the daily cycle [18],[19], contributing to building energy efficiency. The other industrial fields of PCMs, acting as latent heat storage materials are solar water heating systems, photovoltaic panels, or battery thermal management [20].

Thermoregulators involving PCM materials operate similarly, accumulating the excess Joule heat radiating by hot components. Thermal energy is transferred to the ceramic/glass microcapsule interiors, and heat is then accumulated in PCMs or released to the environment when changing the temperature gradient direction. However, due to the low thermal conductivity coefficient of the ceramic/glass microspherules, the stored heat in PCMs, as internal energy, is gradually released to surroundings, acting as a temperature self-regulation mechanism. Obviously, the system operates efficiently within the heat balance range, not exceeding the characteristic latent heat $Q_L = m \cdot L$.

As mentioned above, polycrystalline ceramics exhibit low thermal conductivity; therefore, the PCM materials listed in Table I can be suitable for developing thermoregulators based on PCMs—thermally resistant shells.

When encapsulating PCMs, the aim is to minimize the microspherule diameters as much as possible, thereby increasing the ratio of the active surface area to the core-shell composite volume. This stimulates the thermodynamic processes, which is crucial for the proper operation of thermoregulators. In addition, silica as a shelling material has gained favor due to its stability of the structure, large specific surface area, easily controlled pore size, and non-toxic nature [21].

Moreover, one should remember that core PCM materials are selected appropriately for their forthcoming applications so that their phase change temperature matches the operating points of the thermoregulator/heat storage devices [22].

Also, the latent heat should be as high as possible, especially in volumetric terms, to minimize the size of the heat storage device. On the other hand, the factor determining the heat release rate from PCM is its thermal conductivity, and the higher the thermal conductivity, the faster the energy storage charges or discharges.

The phase transition stability (supercooling extends the heat release time) and resistivity to heating-cooling cycles significantly prolong the heat reservoir life.

Piotr Zachariasz, Bartłomiej Sikora, Radosław Cichocki, Beata Synkiewicz-Musialska are with Łukasiewicz Research Network–Institute of Micro-electronics and Photonics, Cracow, Poland (e-mail: piotr.zachariasz@imif.lukasiewicz.gov.pl, bartlomiej.sikora@imif.lukasiewicz.gov.pl, radoslaw.cichocki@imif.lukasiewicz.gov.pl, beata.synkiewicz.musialska@imif.lukasiewicz.gov.pl).

Elżbieta Szostak is with Department of Chemistry, Jagiellonian University, Cracow, Poland (e-mail:szostak@chemia.uj.edu.pl).

The work involves Li_2CuPO_4 and $Mg_2Al_3[AlSi_5O_{18}]$ electroceramics and [Luxolina]-TEOS, [Erythritol]-HDPE systems as heat-resistant microspherules. The research concerned the synthesis of Li_2CuPO_4, structural stability evaluation of core-shell PCM composites, and their thermal properties. The aim was also to thermally match electroceramic and phase-change materials to gain passive thermal elements (thermoregulators) for electronics applications.

Fig.1. Synthesis scheme of the [Luxolina]-TEOS composite

TABLE I
THERMAL PARAMETERS OF SELECTED PCM MATERIALS

Material	Melting point [°C]	Latent heat [kJ/kg]
Acetamide	81	241
Stearic acid	69.0	199
Erythritol	117.7	339.8
Paraffins	< 100	~200
$MgCl_2 \cdot 6H_2O$	117	167
$Ba(OH)_2 \cdot 8H_2O$	78	265

II. EXPERIMENTAL DETAILS

Synthesis of Li_2CuPO_4 was carried out by a wet chemistry method (co-precipitation) or by grinding the oxide powders in an agate mortar. In the first approach, a solid precursor ($CuSO_4 \cdot 7H_2O$) was mixed with phosphoric acid (H_3PO_4) in a water-assisted process (30 ml) and then neutralized with an alkaline ingredient (LiOH). The reaction stoichiometry was selected so the molar ratio of Li, Cu, and P ions equal 3:1:1.

The second variant of Li_2CuPO_4 synthesis involved grinding substrates in an agate mortar. Li_2CO_3 and $(NH_4)_2HPO_4$ weighed in 1:1 stoichiometry ratio were mixed for 20 minutes to degasses ammonia. Then, the mixture was calcined at 800 °C for 4 h, grounded, and combined with Cu_2O in a 1:1 weight ratio. The uniaxially pressed pellets were sintered at a temperature of 720 °C for 5 h in protective Al_2O_3 powder to prevent Cu oxidation.

On the other hand, $Mg_2Al_3[AlSi_5O_{18}]$ electroceramics (Cordierite) was synthesized using a solid-state reaction method via ball milling. MgO, Al_2O_3, and SiO_2 weighed in stoichiometric proportions were homogenized in a ball mill (300 rpm) for 6 h. After drying the mixed powder, the pellets were sintered at 1420 °C for 2 h.

In cooperation with the Faculty of Chemistry at Jagiellonian University, commercial microgranulates of phase-change materials (Luxolina paraffin and Erythritol sweetener) were microcapsulated according to a process scheme (Figure 1).

The fabrication of paraffin-SiO_2 microshells involved centrifuging melted paraffin at 70 °C with additions of n-amyl alcohol, EtOH 96% (ethyl alcohol), and TEOS (tetraethyl orthosilicate), followed by stirring for 60 min. Product precipitation was initiated by adding NH_3 (aq), and then [Luxolina]-TEOS composite was washed, vacuum filtered, and slowly dried at 50 °C for 48 h.

In turn, [Erythritol]-HDPE microspherules were prepared by solvent-assisted melting infiltration [23],[24]. The starting ingredients were dissolved in xylene at 120 °C by continuous stirring for three hours to thoroughly soak the Erythritol into HDPE. The mixture was then dried at 100 °C for 12 h to extract the xylene remains from the composite.
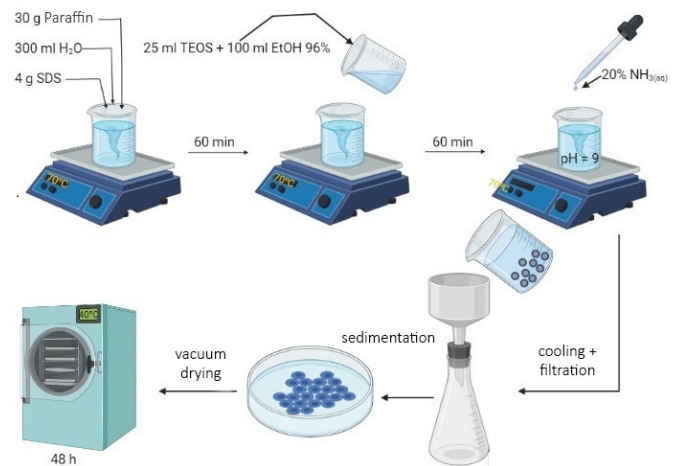
Structural analysis of ceramic sinters was carried out on a Bruker D8 Advance ECO powder diffractometer equipped with a copper X-ray source ($\lambda_{K\alpha} = 1.5406$ Å) and heating chamber for in-situ XRD up to 1500 °C. Diffraction patterns were collected in Bragg-Brentano geometry in a $15 \div 70$ range of 2θ angles.

SEM imaging was carried out using a Quattro S electron microscope from Thermo Fisher Scientific equipped with a field emission electron gun (FEG), an EDXS (Energy-Dispersive X-ray Spectroscopy) detector, and operating at various vacuum modes (HV, ESEM, and LV). SEM microimages were taken using ETD(SE), LVD, and DBS(CBS) detectors in accelerating voltages of $10 \div 30$ kV and magnifications of $2\,000 \div 25\,000$ x.

The thermal properties were evaluated at two testing stations by enrolment of thermal effects related to Joule heat flow generated by current-voltage sources. The first station was a one-side heated quasi-isotropic system with an infrared camera (IR-CAM) mounted above the sample-Peltier unit assembly. The camera recorded real-time temperature on the top surface of specimens. The electrical polarity controlled whether the Peltier unit operated in heating or cooling mode.
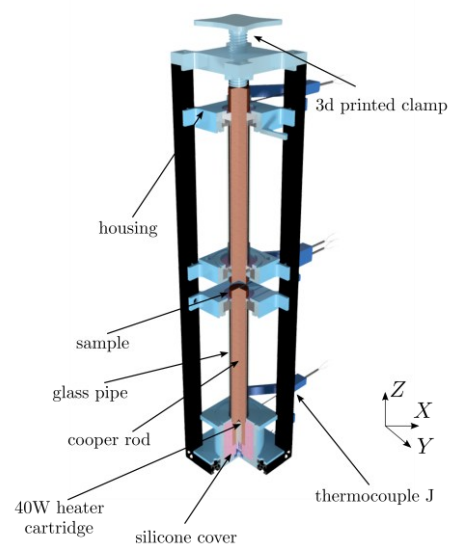

Fig.2. Scheme of the thermal conductivity diagnostic station

The crucial element of the second diagnostic station was two axis-centered copper, between which the sample was fixed in thermal contact (Figure 2). It was a heat pipe thermally isolated from the surroundings using the glass tube, air gap, and Plexiglass elements. Two pairs of thermocouples monitored the heat flow throughout the system. Only time-dependent temperature changes at both ends of the copper rods were analyzed at the current stage. However, the results will be used in future considerations of various thermal energy transport models.

III. RESULTS AND DISCUSSION

Figure 3 shows the XRD patterns of the Cordierite and Li-Cu-P-O system. Cordierite crystallizes in a highly symmetric orthorhombic phase (*Cccm*, No. 66) characterized by narrow Bragg reflections (Figure 3a) and a unit cell size of $a = 17.194$ Å, $b = 9.813$ Å, and $c = 9.346$ Å, respectively. For Li_2CuPO_4, sintering between 700 and 800 °C is sufficient to initiate the synthesis of lithium copper phosphate (Figure 3b,c). However, Li_2CuPO_4 single-phase is technologically challenging, as at least one impurity phase co-exists at each synthesis stage.
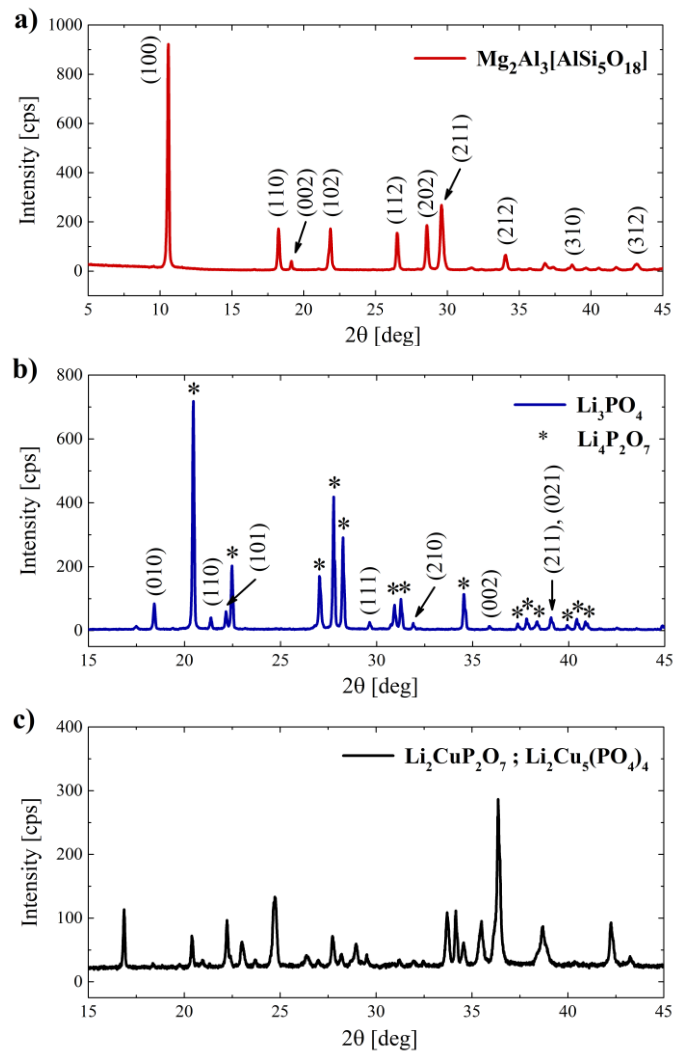
Fig.3. XRD pattern of (a) Cordierite and (b, c) Li-Cu-P-O synthesis stages - prevalent intermediate Li_3PO_4 phase, and a mixture of $Li_2CuP_2O_7$ and $Li_2Cu_5(PO_4)_4$ phases

Figure 4 presents SEM microimages of all investigated materials. Electroceramic sinters were explored by local microstructure homogeneities, porosity degrees, and crystallite sizes. On the other hand, PCMs were characterized according to the size and shape of micro-spherules and encapsulation efficiencies.
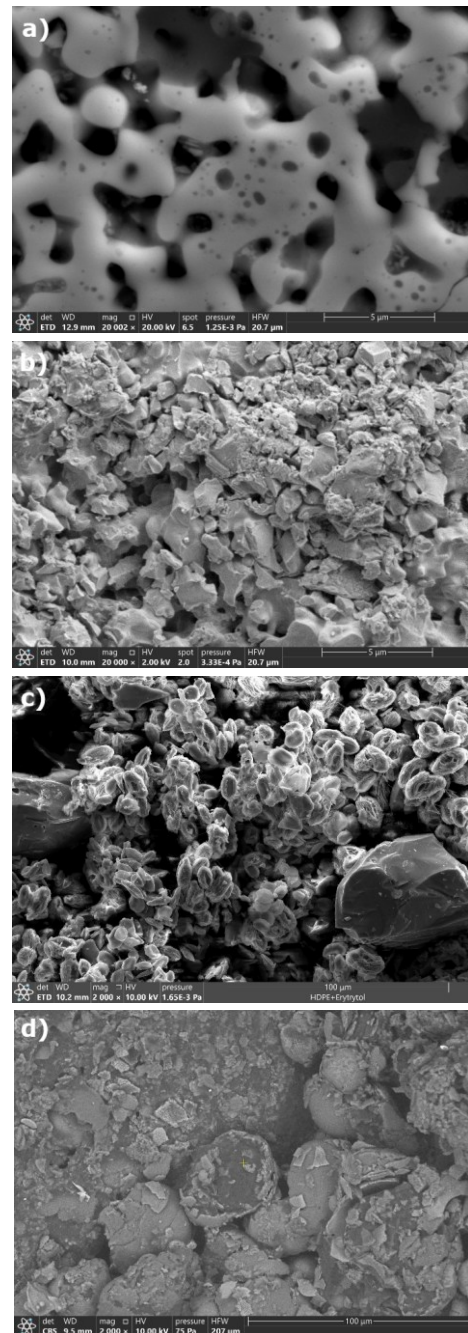
Fig.4. SEM micrographs of (a) Li-Cu-P-O and (b) Cordierite sinters, as well as (c) [Luxolina]-TEOS and (d) [Erythritol]-HDPE core-shells

Cordierite pellet reveals waterproofness due to a strongly condensed local microstructure (Figure 4a) with tightly adjacent grains in sizes $1 \div 4$ μm. Moreover, the fracture surface of the Cordierite pellet presents a low degree of porosity and the decoration of large grains with smaller crystallites ($0.25 \div 0.5$ μm), making the local microstructure more heterogeneous.

In turn, SEM imaging was carried out on the Li-Cu-P-O metallographic surface, showing multi-level porosity (Figure 3b). The grains of lithium copper phosphate are very irregular, favoring numerous voids in the local microstructure. Furthermore, sealed pores inside the crystallites ($0.2 \div 1.0$ μm) demonstrate a substantial air phase in the sinter (Figure 4b).

The above behavior exhibits the difficulty of removing gaseous products (NH_3, CO_2) during the Li_2CuPO_4 synthesis. At the same time, a high porosity level, e.g., promotes effective graduation of dielectric properties for sinters from the lithium copper phosphate family. It is worth mentioning that for $LiCuPO_4$ (Cu^{2+}), the relative permittivity $\varepsilon_R = 5.2$ [25].

SEM experiment also illustrated the encapsulation of PCMs in organic microshells. It was shown that [Erythritol]-HDPE is a core-shell composite, where the polypropylene tightly surrounded the food sweetener grains, forming spindle-shaped, feathery crystallites with average sizes of $12 \div 20$ μm in longer diagonal (Figure 4c).

Despite a formation of [Luxolina]-TEOS microspherules with an estimated 50 μm size, satisfactory paraffin trapping in TEOS was not fetched (Figure 4d) since micro-shells were semi-open, heavily cracked, and decorated with numerous small fragments. Moreover, a considerable PCM outflow into the microstructure pores was observed, suggesting difficulties in the TEOS micro-shell embrittlement and paraffin encapsulation.

Thermal characteristics extracted from the semi-open diagnostic system (Figure 5) showed that heating or cooling to set temperatures was approximately three times shorter for electroceramics than for PCM specimens (Table II). It is a crucial result since Cordierite and Li-Cu-P-O system are good thermal resistivity elements.

Therefore, the heating rate index (f_h) is several times less for PCM material (Figure 5c), indicating thermal energy accumulation as latent heat at a phase transition. Even though high-porosity Li-Cu-P-O strongly dissipates the Joule heat, it still heats up faster than PCM (Table II).
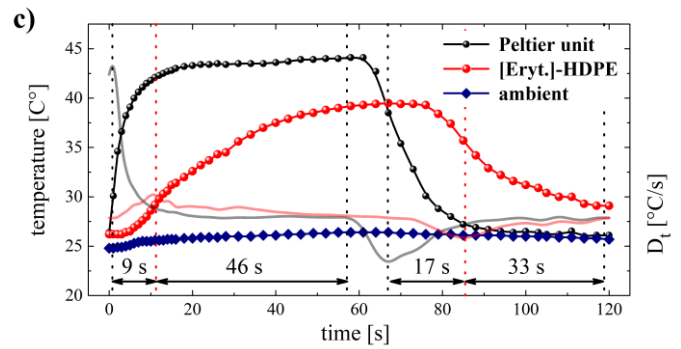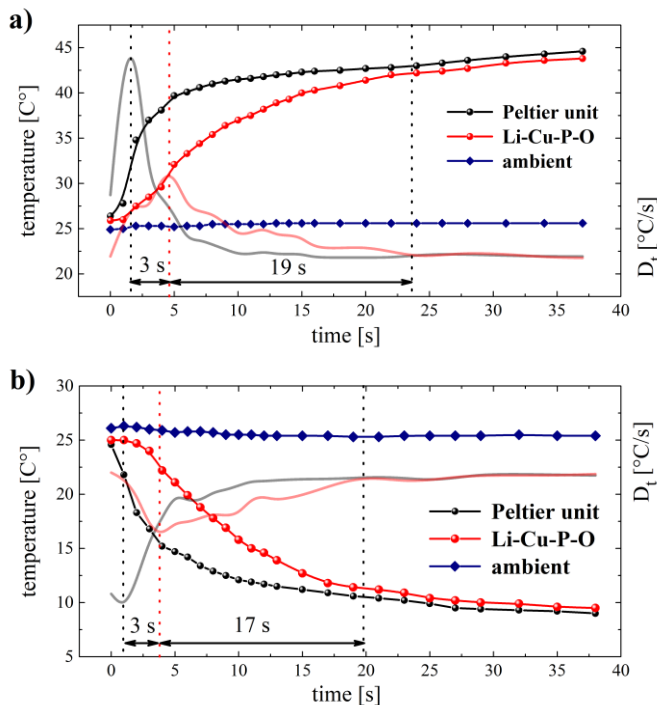
a)

b)

c)

Fig.5. Thermal curves and time derivatives of Li-Cu-P-O ceramics gathered in the contact method at (a) heating and (b) cooling modes. For comparison, thermal characteristics for (c) [Erythritol]-HDPE composite

TABLE II
THERMAL CHARACTERISTICS

System	t_s [s]	f_h [°C/s]	j_h [s]
Cordierite	20	2.5	3
Li-Cu-P-O	23	2.1	3
[Erythritol]-HDPE	55	0.25	9

t_s - temperature stability time, f_h - heating rate index, j_h - heating lag factor

The heating lag factor (j_h) was also extracted as a spread of derivative maxima on the time scale for the Peltier unit and specimen (Figure 5). The above parameter is a temperature increase delay in the specimen while absorbing heat energy. The j_h parameter was three times longer for the [Erythritol]-HDPE composite than for electroceramic samples (Table II)

Similarly to IR-CAM inspection, the axial flow of thermal energy was observed in a 1-D system of two Cu rods and a disk-shaped specimen (Figure 2).

For reference ceramics (AlN), with thermal conductivity comparable to copper, the heat flow was saturated after 8 minutes (Figure 6c,d). The differences of $t_1 - t_0 = 43$ °C, $t_2 - t_1 = 37$ °C, and $t_3 - t_2 = 17$ °C indicate a temperature gradient driving heat flow in the system.

The heat conductivity curves of [Erythritol]-HDPE are entirely different (shell of thermal resistivity and inner heat absorber). Heat flow was not fixed during the 17 minutes of the experiment, as it was limited due to the HDPE melting point at 131 °C. The above characteristic resulted in closely related t_0 and t_1 temperatures monitored at the first Cu rod (Figure 6c,d) due to the thermal resistivity of [Erythritol]-HDPE preventing the heat transfer to the second Cu rod.

Moreover, even though the diagnostic installation was constantly supplied with Joule heat (40 W), no temperature saturation was observed, which either arises over a longer period due to the high thermal capacity of Cu rods or the heat propagation mechanism is more intricate.

CONCLUSION

Isolating Li_2CuPO_4 or $LiCuPO_4$ [25] as a single-phase was challenging regardless of the synthesis route (solid-state reaction or wet chemical method). Nevertheless, the Li-Cu-P-O system was characterized structurally and in dielectric and thermal properties.

The Cordierite sinter and Li-Cu-P-O electroceramics properties were consistent in thermal conductivity with HDPE

microspherules (encapsulators) protecting phase-change material (Erythritol). In turn, the [Luxolina]-TEOS composite requires more satisfactory encapsulation.

In the next step, investigated ceramics with functional PCM elements will be integrated to assemble active components for temperature stabilization. Furthermore, axial heat flow modeling, considering conductance, convection, and radiation components, is scheduled for discussed ceramic materials.

It seems that electroceramics with embedded phase-change materials, as investigated in this work, could potentially be used to design passive thermal stabilizers in high-performance electronic systems.
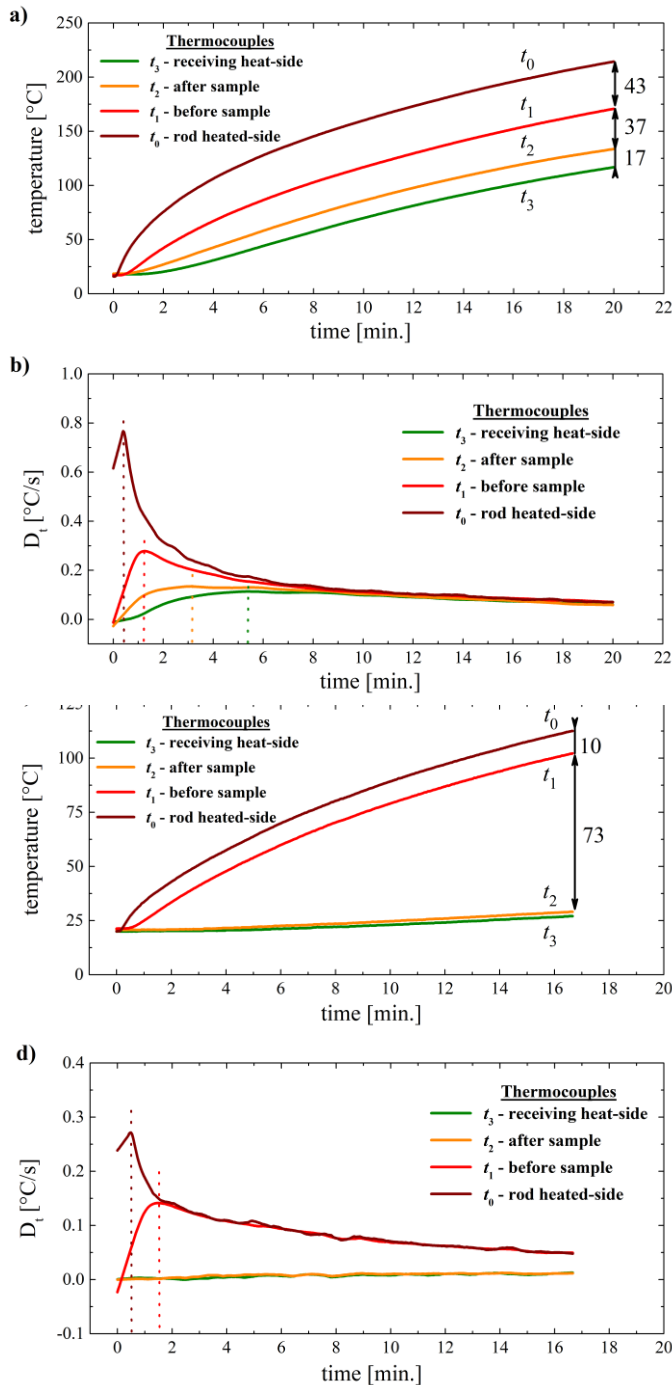

Fig.6. Thermal curves and time derivatives of (a, b) reference AlN and (c, d) [Erythritol]-HDPE composite collected at the heat flow experiment

References

[1] V. Bianco, M. De Rosa, K. Vafai, "Phase-change materials for thermal management of electronic devices", Appl. Therm. Eng., vol. 214, pp. 118839, 2022. https://doi.org/10.1016/j.applthermaleng.2022.118839

[2] Z. Khan, "A review of phase change materials (PCMs) in electronic device cooling applications", Future Technology, vol. 1, no. 2, pp. 36-45, 2022.

[3] Y. Yao, W. Li, J. Liu, Z. Deng, "Liquid metal phase change materials for thermal management of electronics", Adv. Phys.: X, vol. 9, no. 1, pp. 1-48, 2024. https://doi.org/10.1080/23746149.2024.2324910

[4] B. Praveen, S. Suresh, V. Pethurajan, "Heat transfer performance of graphene nano-platelets laden microencapsulated PCM with polymer shell for thermal energy storage based heat sink", Appl. Therm. Eng., vol. 156, pp. 237-249, 2019. https://doi.org/10.1016/j.applthermaleng.2019.04.072

[5] R. Li, Y. Zhou, X. Duan, "Nanoparticle enhanced paraffin and tailing ceramic composite phase change material for thermal energy storage", Sustainable Energy Fuels, vol. 4, pp. 4547-4557, 2020

[6] Y. Huang, A. Stonehouse, Ch. Abeykoon, "Encapsulation methods for phase change materials – A critical review", Int. J. Heat Mass Transf., no. 200, pp. 123458, 2023. https://doi.org/10.1016/j.ijheatmasstransfer.2022.123458

[7] A. Palacios, M.E. Navarro-Rivero, B. Zou, Z. Jiang, M.T. Harrison, Y. Ding, "A perspective on Phase Change Material encapsulation: Guidance for encapsulation design methodology from low to high-temperature thermal energy storage applications", J. Energy Storage, no. 72, pp. 108597, 2023. https://doi.org/10.1016/j.est.2023.108597

[8] Y. Chang, X. Yao, Y. Chen, L. Huang, D. Zou, "Review on ceramic-based composite phase change materials: Preparation, characterization and application", Compos. B Eng., Vol. 254, pp. 110584, 2023. https://doi.org/10.1016/j.compositesb.2023.110584

[9] Q. Ma, D. Zou, Y. Wang, K. Lei, "Preparation and properties of novel ceramic composites based on microencapsulated phase change materials (MEPCMs) with high thermal stability", Ceram. Int., vol. 47, no. 17, pp. 24240-24251, 2021. https://doi.org/10.1016/j.ceramint.2021.05.135

[10] D. Galusek, D. Galusková, "Alumina matrix composites with non-oxide nanoparticle addition and enhanced functionalities", Nanomaterials, vol. 5, no.1, pp.115-143, 2015. https://doi.org/10.3390/nano5010115

[11] J. Paterson, D. Singhal, D. Tainoff, J. Richard, O. Bourgeois, "Thermal conductivity and thermal boundary resistance of amorphous Al_2O_3 thin films on germanium and sapphire", J. Appl. Phys., vol. 127, no.24, pp. 245105, 2020. https://doi.org/10.1063/5.0004576

[12] S.S. Chen, Q.Z. Wu, C. Mishra, J.Y. Kang, H.J. Zhang, K.J. Cho, W.W. Cai, A.A. Balandin, R.S. Ruoff, "Thermal conductivity of isotopically modified graphene", Nat. Mater., vol. 11, pp. 203-207, 2012. https://doi.org/10.1038/nmat3207

[13] E. Pop, D. Mann, Q. Wang, K. Goodson, H. Dai, "Thermal conductance of an individual single-wall carbon nanotube above room temperature", Nano Lett., vol. 6, no.1, pp. 96-100, 2006. https://doi.org/10.1021/nl052145f

[14] D. Xia, H. Li, P. Huang, "Understanding the Joule-heating behaviors of electrically-heatable carbon-nanotube aerogels", Nanoscale Adv., vol. 3, pp. 647-652, 2021. https://doi.org/10.1039/D0NA01002B

[15] I. Afaynou, H. Faraji, K. Choukairy, A. Arshad, M. Arici, "Heat transfer enhancement of phase-change materials (PCMs) based thermal management systems for electronic components: A review of recent advances", Int. Commun. Heat Mass Transf., vol. 143, pp. 106690, 2023. https://doi.org/10.1016/j.icheatmasstransfer.2023.106690

[16] J. Yuan, K. Yang, B. Huang, J. Li, C. Qiu, Y. Jiang, "Transient thermal management of laser systems using Plate-Fin phase change heat Exchangers: Experimental and computational study", Appl. Therm. Eng., vol. 255, pp. 123994, 2024. https://doi.org/10.1016/j.applthermaleng.2024.123994

[17] D.X. Zhang, C.Y. Zhu, L. Gong, B. Ding, M.H. Xu, "Investigation on thermal performance of a novel passive phase change material-based fin heat exchanger", J. Therm. Sci. Eng. Appl., vol. 15, no. 2, pp. 021007, 2023. https://doi.org/10.1115/1.4056009

[18] V.D. Cao, S. Pilehvar, C. Salas-Bringas, A.M. Szczotok, J.F. Rodriguez, M. Carmona, N. Al-Manasir, A.L. Kjøniksen, "Microencapsulated phase change materials for enhancing the thermal performance of Portland cement concrete and geopolymer concrete for passive building applications", Energy Convers. Manag., vol. 133, pp. 56-66, 2017. https://doi.org/10.1016/j.enconman.2016.11.061

[19] A. Sivanathan, Q. Dou, Y. Wang, Y. Li, J. Corker, Y. Zhou, M. Fan, "Phase change materials for building construction: An overview of nano-/micro-encapsulation", Nanotechnol. Rev., vol. 9, no.1, pp. 896-921, 2020. https://doi.org/10.1515/ntrev-2020-0067

[20] V.J. Reddy, M.F. Ghazali, S. Kumarasamy, "Innovations in phase change materials for diverse industrial applications: A comprehensive review", Results in Chemistry, vol. 8, pp. 101552, 2024. https://doi.org/10.1016/j.rechem.2024.101552

[21] Z. Xiangfa, X. Hanning, F.Jian, Z. Changrui, J. Yonggang, "Preparation and thermal properties of paraffin/porous silica ceramic composite", Compos. Sci. Technol., vol. 69, pp. 1246-1249, 2009. https://doi.org/10.1016/j.compscitech.2009.02.030

[22] K. Yu, Y. Wang, Y. Li, J. Baleta, J. Wang, B. Sundén, "Effect of phase change materials on heat dissipation of a multiple heat source system",

Open Phys., vol. 17, pp. 797-807, 2019. https://doi.org/10.1515/phys-2019-0083

[23] S. Jaiswal, S. Sonare, P. Mahanwar, "Review on phase change material and its composites with polyolefins", Int. J. Novel Res. Devel., vol. 8, no. 2, pp. 228-244, 2023. ISSN: 2456-4184

[24] S. Chai, K. Sun, D. Zhao, Y. Kou, Q. Shi, "Form-Stable Erythritol/HDPE Composite Phase Change Material with Flexibility, Tailorability, and High Transition Enthalpy", ACS Appl. Polym. Mater., vol. 2, no. 11, pp. 4464–4471, 2020. https://doi.org/10.1021/acsapm.0c00584

[25] B. Synkiewicz-Musialska, P. Zachariasz, E. Szostak, "Synthesis and thermal stabilization properties of phase change materials and their application in the composite with LiCuPO$_4$", Proceedings of the 4th International Conference on Micro-electronic Devices and Technologies (MicDAT '2022), IFSA Publishing, S. L., Barcelona, Spain, ISBN: 978-84-09-43856-3